Journal of Power Sources 196 (2011) 6951–6955

Contents lists available at ScienceDirect

Journal of Power Sources

journal homepage: www.elsevier.com/locate/jpowsour

Short communication

# A nano-structured and highly ordered polypyrrole-sulfur cathode for lithium–sulfur batteries

Xiao Liang, Yu Liu, Zhaoyin Wen*, Lezhi Huang, Xiuyan Wang, Hao Zhang

*CAS Key Laboratory of Materials for Energy Conversion, Shanghai Institute of Ceramics, Chinese Academy of Sciences, Shanghai 200050, PR China*

ARTICLE INFO

*Article history:*
Received 26 August 2010
Received in revised form
22 November 2010
Accepted 23 November 2010
Available online 30 November 2010

*Keywords:*
Sulfur
Tubular polypyrrole
Lithium–sulfur battery
Composite cathode

ABSTRACT

A tubular polypyrrole (T-PPy) fiber is synthesized as a conductive matrix for the cathode of lithium–sulfur secondary battery. The sublimed sulfur is incorporated with the T-PPy by a co-heating process. The location and the content of sulfur show a significant effect on the electrochemical behavior of the composite. A reversible capacity of ca. 650 mAh $g^{-1}$ is maintained for over 80 cycles for the S/T-PPy composite with 30 wt.% sulfur. The enhanced conductivity, the favorable distribution of the nano-sized sulfur in the T-PPy and the stable retention of polysulfides lead to the improvement of the cycling stability of the sulfur based electrode.

© 2010 Elsevier B.V. All rights reserved.

## 1. Introduction

Rechargeable lithium/sulfur (Li/S) battery shows a high theoretical capacity of 1675 mAh $g^{-1}$, which is nearly one magnitude higher than that of the currently commercialized $LiFePO_4$-based Li-ion battery [1–4]. Sulfur also has the advantages of low cost, low toxicity and abundance as the cathode material [5]. However, poor electrical conductivity of sulfur and intrinsic sulfide shuttle seriously hinder the development of Li/S battery [6,7]. The lithium polysulfides generated during the charge/discharge process is soluble in organic electrolyte, which leads to the loss of the active material in the cathode [8]. Moreover, the soluble polysulfides deposit on the surface of the anode by a shuttle mechanism, which aggravates the corrosion of the anode and increases the internal resistance of the cell, resulting in a rapid fading of the reversible capacity [9]. Many efforts have been devoted to improve the cycling stability of the Li/S battery, mainly focusing on the combination of a conductive matrix with sulfur to form a highly conductive composite. Mesoporous carbon, acetylene black and multiwalled carbon tube have been reported as an absorbing and conducting matrix for sulfur electrode due to their highly porous structure and good electronic conductivity [10–12]. Polypyrrole is another conductive polymer with good compatibility with sulfur and organic electrolytes [13,14]. The morphology of polypyrrole represents a key to improve the electrochemical performance of sulfur. In this study, a tubular polypyrrole (T-PPy) was proposed as the conductive matrix. The S/T-PPy composites were prepared by co-heating the sublimed sulfur with the tubular PPy at a suitable temperature. The electrochemical behaviors of the S/T-PPy composites were investigated.

## 2. Experimental

The tubular polypyrrole (T-PPy) was synthesized by a self-degraded template method [15]. 210 ml aqueous solution of $FeCl_3$ (10.5 mmol) and methyl orange (1.05 mmol) was prepared as the template. 10.5 mmol pyrrole was added into the template and stirred for 24 h. The product was washed by water and ethanol alternatively until the filtrate was colorless. The as-obtained tubular PPy was further dried under vacuum at 50 °C for 12 h. Mixtures of sulfur and the tubular PPy in the weight ratio of 1:1 and 1.5:1 were co-heated at 150 °C for 3 h. During the heating process, the sulfur was molten and filled to the holes of the tubular PPy. The mixtures were further heated at 300 °C for 2 h to vaporize the sulfur remained on the outside surface of the tubular PPy. Two types of S/T-PPy composites with 30 wt.% and 50 wt.% sulfur were prepared, respectively, as reported in Ref. [13]. The processes were performed in Ar atmosphere. Phase of the samples was characterized by X-ray diffraction (XRD, Rigaku RINT-2000) with Cu Kα radiation. Structure of the composites was characterized by FTIR. Morphology of the as-prepared composites was observed by field emission scanning electron microscope (FESEM JSM-6700) and transmission electron microscope (TEM JEM-2010). Thermogravimetry-differential scanning calorimetry (TG-DSC, NETZSCH 409PC) was involved in

* Corresponding author. Tel.: +86 21 52411704; fax: +86 21 52413903.
*E-mail addresses:* yuliu@mail.sic.ac.cn (Y. Liu), zywen@mail.sic.ac.cn (Z. Wen).

0378-7753/$ – see front matter © 2010 Elsevier B.V. All rights reserved.
doi:10.1016/j.jpowsour.2010.11.132

determining the sulfur contents in the S/T-PPy composites. The $N_2$ sorption measurement was performed using Micromeritics Tristar 3000 at 77 K, and specific surface area was calculated using the Brunauer–Emmett–Telley (BET).

The mixtures of 50 wt.% composite, 30 wt.% acetylene black and 20 wt.% PEO binder were added into acetonitrile to form uniform slurries. The slurries were cast onto aluminum foils. After the solvent evaporated, the electrode film was cut to sheets with 14 mm in diameter and further dried at 50 °C under vacuum for 12 h. The pristine sulfur cathode with 30 wt.% sulfur, 50 wt.% acetylene black and 20 wt.% PEO binder was prepared by the same way for comparison. CR2025 type coin cells were assembled in a glove box with oxygen and water contents less than 1 ppm. A solution of 1 M $LiCF_3SO_3$ dissolved in TEGDME was employed as the electrolyte. Celgard 2400 was used as the separator and lithium foils as both the counter and reference electrodes. AC impedance of the cell was measured by a Frequency Response Analyzer (FRA) technique on a Autolab Electrochemical Workstation over the frequency rang from 1 MHz to 10 mHz with the amplitude of 10 mV. The galvanostatic charge and discharge test was carried out using a LAND CT2001A battery test system in a voltage range of 1.0–3.0 V vs. $Li/Li^+$ at a current density of 0.1 mA $cm^{-2}$.

## 3. Results and discussion

Figs. 1a and 2a show respectively the SEM and TEM graphs of the as prepared PPy fibers. As seen, the fibers have a tubular morphology with about 300 nm in outer-diameter and 250 nm in inner-diameter. Such a structure is favorable for the loading of the molten sulfur. SEM and TEM microstructures in Figs. 1a-b and 2a-b show that no significant morphological difference between the S/T-PPy composite with 30 wt.% sulfur and the pristine tubular PPy was observed. It supposed that the sublimed sulfur was possibly restricted within the hollow of the PPy. Filling amount of sulfur has a significant influence on the morphology of the S/T-PPy composites. Different from the composite with 30 wt.% sulfur, the composite with 50 wt.% sulfur displayed obvious irregular agglomeration of sulfur on the outer surface of the PPy tubes, as shown in Figs. 1c and 2c, indicating the saturation of the sublimed sulfur for the hollow of the PPy tubes.

The locations of sulfur in the composites were also roughly proved by BET surface area measurements. Surface areas of the tubular PPy or composites were analyzed through $N_2$ adsorption/desorption measurements at 77 K, as shown in Fig. 3. As the PPy tube was incorporated with sulfur, the surface area decreased obviously. The calculation based on density of sulfur (2.07 g $cm^{-3}$) and pore volume of the tubular PPy (0.241 $cm^3$ $g^{-1}$) shows that 1 g of PPy tube can accommodate 0.498 g sulfur (2.07 g $cm^{-3}$ × 0.241 $cm^3$ $g^{-1}$). It ensures a maximum sulfur content of 33.2 wt.% in the PPy tube. Although parts of the sulfur could be located outer of the PPy tube as the sulfur in the S/T-PPy composite is large than 33.2%, large amount of sulfur should possibly be filled into the PPy tube.

Fig. 4 shows the XRD patterns of the sublimed sulfur and the S/T-PPy composites with different amounts of sulfur. As seen, the S/T-PPy composite with 30 wt.% sulfur has a very broad reflection peak, indicating an amorphous feature of the sulfur in the composite. During the co-heating process at 150 °C, the molten sulfur could possibly penetrate into the hollow PPy of the nano-tubes due to the capillary force and the strong absorbability of PPy to sulfur, which finally formed a homogenous composite [16]. At a higher temperature, e.g. at 300 °C, sulfur coated on the outer surface of the PPy tubes would evaporate. However, when the sulfur content was higher than 30 wt.%, part of the sulfur crystallized on the outer surface of the tubular PPy. Fig. 3b shows the reflection peak of the crystalline sulfur of the S/T-PPy composite with 50 wt.% sulfur.

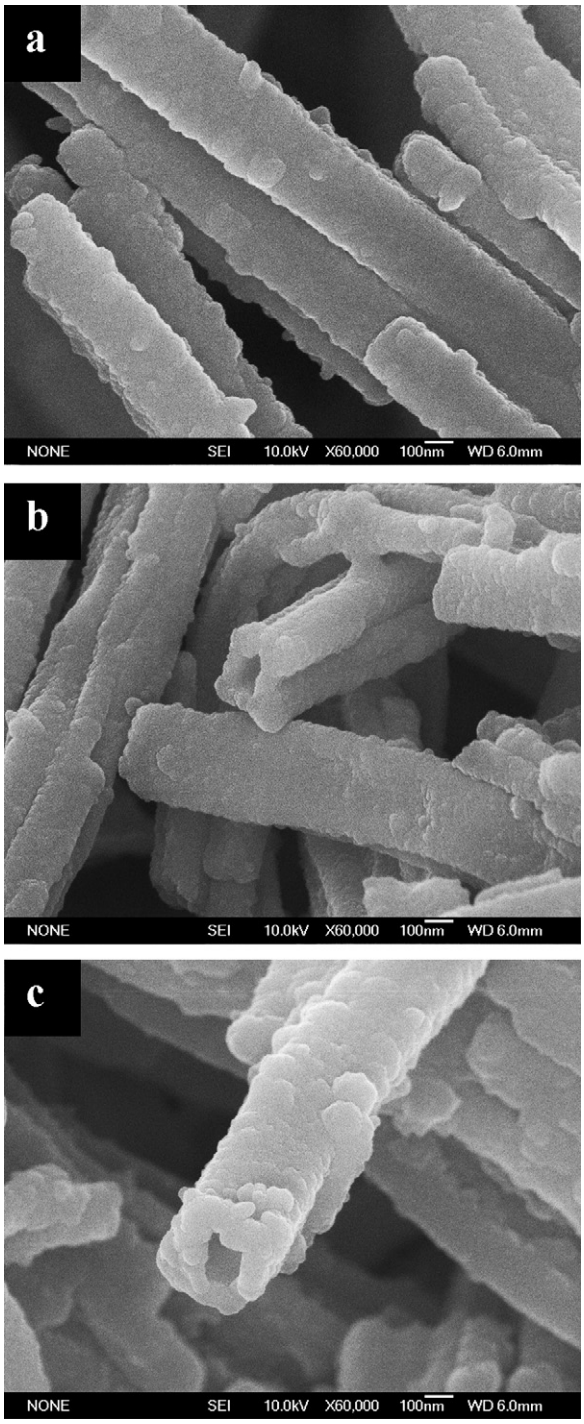


**Fig. 1.** SEM micrographs of the T-PPy (a), the S/T-PPy composite with 30 wt.% sulfur (b) and the S/T-PPy composite with 50 wt.% sulfur (c).

FTIR measurement was further conducted on the composites and the tubular PPy to indicate a possible structure change of the PPy matrix during the co-heating process with sulfur. As shown in Fig. 5, all the three samples exhibited the characteristic bands of PPy, involving the pyrrole ring fundamental vibration at 1545 $cm^{-1}$ and 1458 $cm^{-1}$, the =C–H in-plane vibration at 1291 $cm^{-1}$ and 1043 $cm^{-1}$ and the C–N stretching vibration at 1175 $cm^{-1}$. This is consistent with Ref. [14]. It is indicated that no chemical reaction between sulfur and PPy happened during the co-heating process.

The discharge curves of the S/T-PPy composite with 30 wt.% sulfur are shown in Fig. 6. Two voltage plateaus at about 2.4 V and

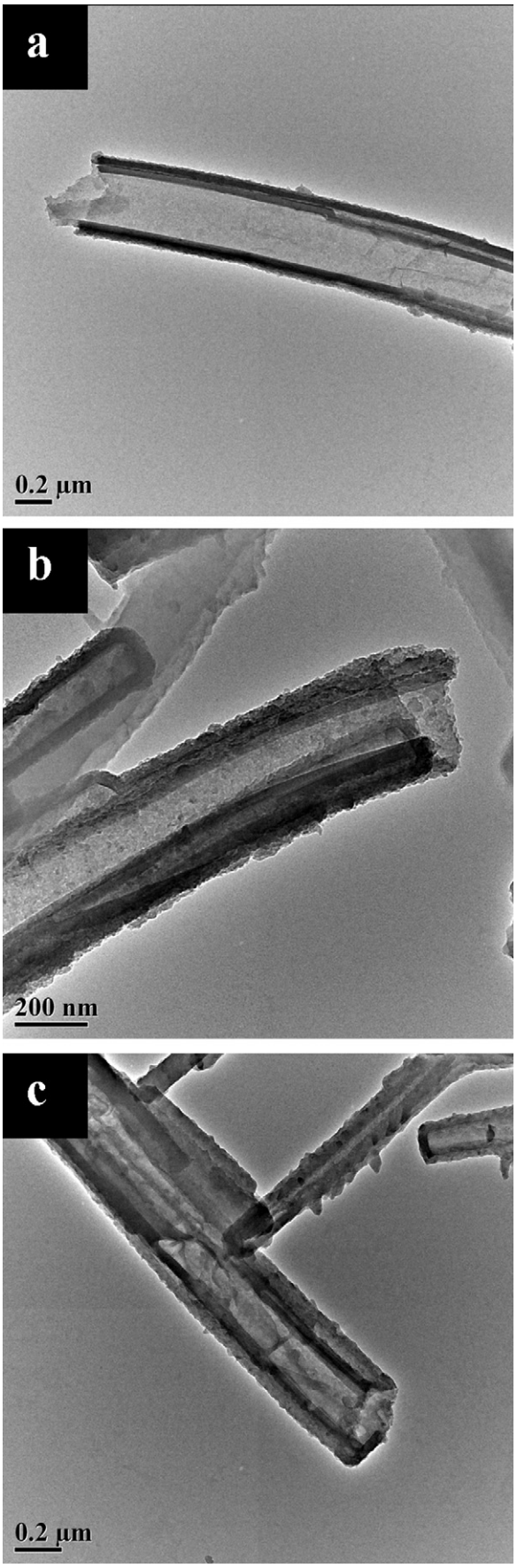


**Fig. 2.** TEM micrographs of the T-PPy (a), the S/T-PPy composite with 30 wt.% sulfur (b) and the S/T-PPy composite with 50 wt.% sulfur (c).

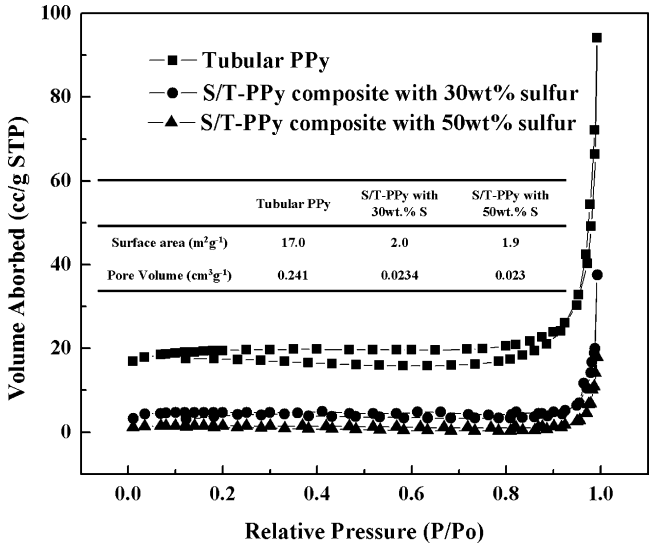


**Fig. 3.** Nitrogen sorption isotherms of tubular PPy and the S/T-PPy composites; inserts shows the surface areas and pore volumes.

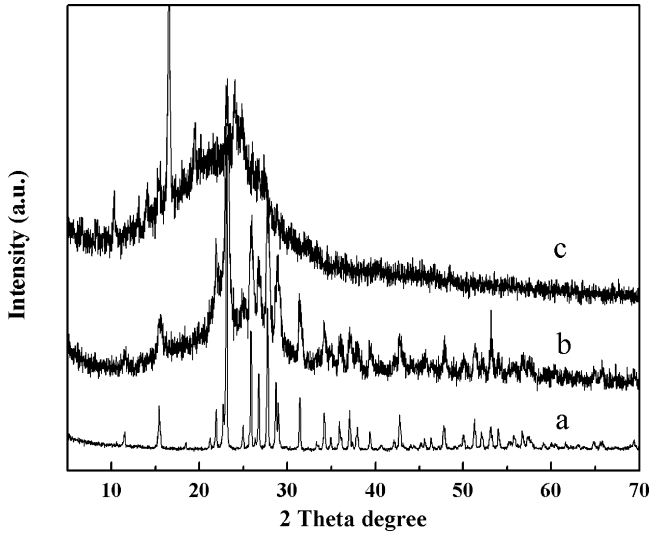


**Fig. 4.** XRD patterns of the sublimed sulfur (a), the S/T-PPy composite with 50 wt.% sulfur (b) and the S/T-PPy composite with 30 wt.% sulfur (c).

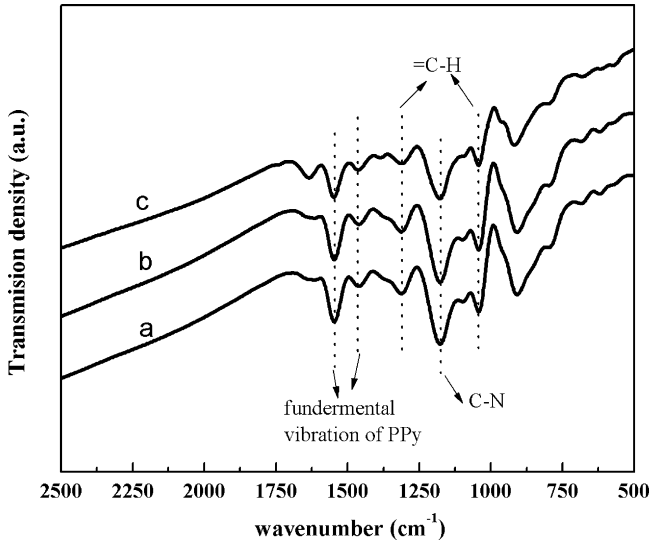


**Fig. 5.** FTIR spectra of the T-PPy (a), the S/T-PPy composite with 30 wt.% sulfur (b) and the S/T-PPy composite with 50 wt.% sulfur (c).

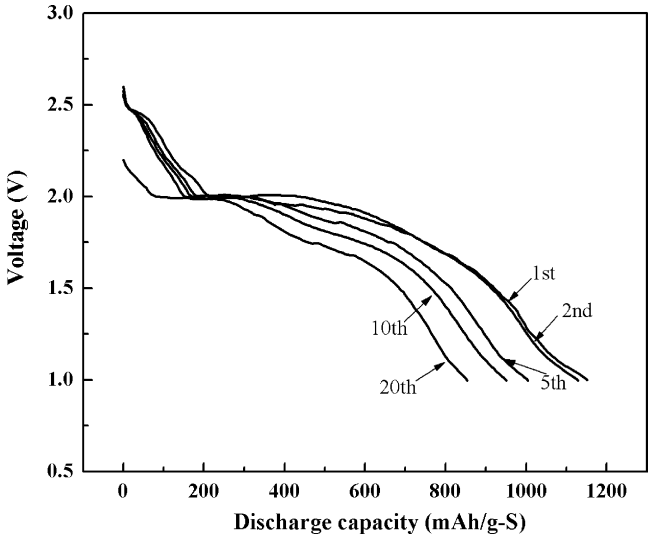


**Fig. 6.** Discharge curves of the S/T-PPy composite with 30 wt.% sulfur.

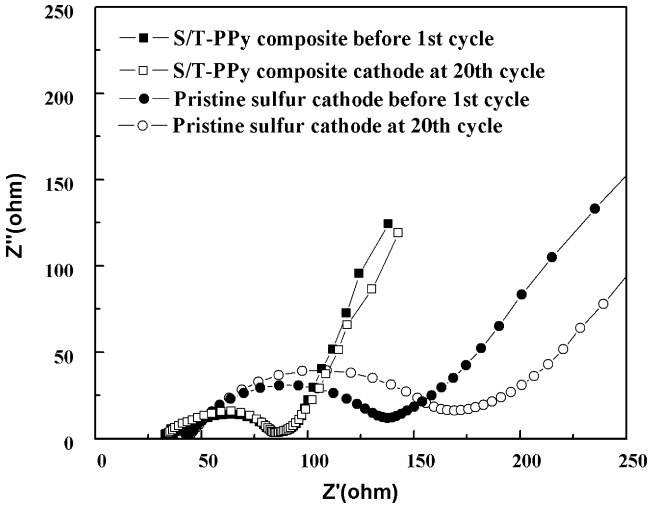


**Fig. 8.** AC impedance spectra of the S/T-PPy composite with 30 wt.% sulfur and pure sulfur electrodes.

2.0 V were observed for all the cycles. The 2.4 V plateau is caused by the changes from element sulfur to higher-order lithium polysulfides ($Li_2S_n$, $n \geq 4$). The 2.0 V plateau is related to the reduction of higher-order polysulfides to lower-order polysulfides ($n < 4$) [17]. As seen, the composite shows a good reversibility with an initial discharge capacity as high as ca. 1151.7 mAh $g^{-1}$. The favorable electrochemical performances of the composite could be attributed to the as-proposed microstructure, with nano-sized sulfur and the highly dispersive lithium polysulfides trapped in the hollow of the PPy tubes.

Fig. 7 shows the cycling performance of the S/T-PPy composites and the pristine sulfur electrodes. As seen, the cycling stability of the S/T-PPy composite with 30 wt.% sulfur is obviously superior to that of the composite with 50 wt.% sulfur and the pristine sulfur electrode. The composite with 30 wt.% sulfur remained a stable capacity of ca. 650 mAh $g^{-1}$ for over 80 cycles. On the contrary, the reversible capacities at the 80th cycle for the pristine sulfur and the composite with 50 wt.% sulfur were only ca. 208 and 140 mAh $g^{-1}$, respectively. As discussed above, for the S/T-PPy composite with 50 wt.% sulfur, large amount of sulfur could cover the surface of the PPy tube. It could hinder the electron path for the active sulfur and therefore speed the capacity fading. Moreover, lithium polysulfides generated from the outer surface sulfur would easily diffuse into the electrolyte, which finally leads to a poor electrochemical behavior. On the other hand, most of the sulfur was homogenously dispersed in the PPy tube for the S/T-PPy composite with 30 wt.% sulfur. The trapped sulfur and the generated polysulfides in the tube were difficult to diffuse out of the tube by capillary forces. It suggested that a suitable content and the location of sulfur would be necessary for a stable cycling performance.

Fig. 8 shows the EIS analysis results of the S/T-PPy composite and the pristine sulfur electrode after different cycles. The semi-circle at high frequency corresponds to the contact and charge transfer resistances. The short inclined line in low frequency region is related to the ion diffusion within the electrodes. It is obvious that both the contact and charge transfer resistances of the S/T-PPy composite with 30 wt.% sulfur were smaller than those of the pristine sulfur electrode, which could be attributed to the enhanced conductivity and the favorable distribution of the nano-sized sulfur in the T-PPy matrix. Compared with the pristine sulfur electrode, the charge transfer resistance of the S/T-PPy composite is much more stable upon cycling. This ensured an improved cycling performance of the composite.

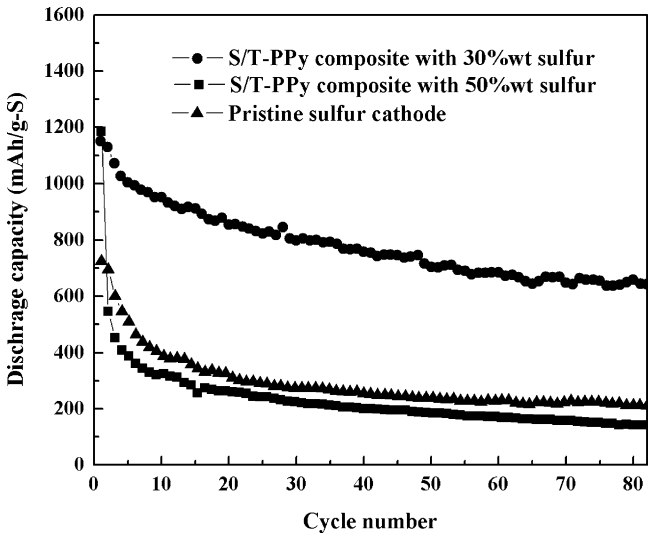


**Fig. 7.** Cycling performance of the composites and the pristine sulfur electrodes.

## 4. Conclusion

Sulfur was penetrated into the tubular PPy fibers by capillary forces during a co-heating process. The conductivity of the composite was significantly improved by the tubular PPy matrix. An initial discharge capacity of ca. 1151.7 mAh $g^{-1}$ is displayed for the S/T-PPy composite with 30 wt% sulfur, and nearly a constant capacity of ca. 650 mAh $g^{-1}$ after 80 cycles. It was suggested that the improvement of the cycling stability of the S/T-PPy composite was mainly attributed to the improved conductivity, the favorable distribution of the nano-sized sulfur in the tubular PPy matrix and the excellent retention of the polysulfides within the electrode.

## Acknowledgements

This work was financially supported by NSFC Project No. 50730001 and 50973127; research projects of Chinese Science and Technology Ministry No. 2007BAA07B01 and No. 2007CB209700; research projects from the Science and Technology Commission of Shanghai Municipality No. 08DZ2210900 and No. 09PJ1410800.

## References


[1] W. Zheng, Y.W. Liu, X.G. Hu, C.F. Zhang, Electrochim. Acta 51 (2006) 1330.
[2] D. Marmorstein, T.H. Yu, K.A. Striebel, F.R. McLarnon, J. Hou, E.J. Cairns, J. Power Sources 89 (2000) 219.
[3] N. Petr, M. Klaus, K.S.V. Santhanam, H. Otto, Chem. Rev. 97 (1997) 207.
[4] C. Delacourt, P. Poizot, J.M. Tarascon, C. Masquelier, Nature Mater. 4 (2005) 254–260.
[5] H. Yamin, E. Peled, J. Power Sources 9 (1983) 281.
[6] X.L. Ji, K.T. Lee, L.F. Nazar, Nature Mater. 8 (2009) 500.
[7] J. Wang, S.Y. Chew, Z.W. Zhao, S. Ashraf, D. Wexler, J. Chen, S.H. Ng, S.L. Chou, H.K. Liu, Carbon 46 (2008) 229–235.
[8] L.X. Yuan, J.K. Feng, X.P. Ai, Y.L. Cao, S.L. Chen, H.X. Yang, Electrochem. Commun. 8 (2006) 610–614.
[9] Y.V. Mikhaylik, J.R. Akridge, J. Electrochem. Soc. 151 (11) (2004) A1969–A1976.
[10] C.D. Liang, N.J. Dudeny, J.Y. Howe, Chem. Mater. 21 (2009) 4724–4730.
[11] B. Zhang, C. Lai, Z. Zhao, X.P. Gao, Electrochim. Acta 54 (2009) 3708–3713.
[12] L.X. Yuan, H.P. Yuan, X.P. Qiu, L.Q. Chen, W.T. Zhu, J. Power Sources 189 (2009) 1141–1146.
[13] J. Wang, J. Chen, K. Konstantinov, L. Zhao, S.H. Ng, G.X. Wang, Z.P. Guo, H.K. Liu, Electrochim. Acta 51 (2006) 4634–4638.
[14] M.M. Sun, S.C. Zhang, T. Jiang, L. Zhang, J.H. Yu, Electrochem. Commun. 10 (2008) 1819–1822.
[15] X.M. Yang, Z.X. Zhu, T.Y. Dai, Y. Lu, Macromol. Rapid Commun. 26 (2005) 1736–1740.
[16] C. Lai, X.P. Gao, B. Zhang, T.Y. Yan, Z. Zhou, J. Phys. Chem. C 113 (2009) 4712–4716.
[17] D. Marmorstein, T.H. Yu, K.A. Striebel, E.J. Cairns, J. Power Sources 89 (2000) 219.